

# Study on the Milling of Additive Manufactured Components

Robert Laue \*, Pascal Colditz, Manuel Möckel and Birgit Awiszus

Institute for Machine Tools and Productions Processes, Professorship Virtual Production Engineering, Chemnitz University of Technology, 09126 Chemnitz, Germany; pascal.colditz@mb.tu-chemnitz.de (P.C.); manuel.moeckel@s2018.tu-chemnitz.de (M.M.); birgit.awiszus@mb.tu-chemnitz.de (B.A.)

\* Correspondence: robert.laue@mb.tu-chemnitz.de

**Abstract:** Additive manufacturing of components has increased significantly in capacity; additional post-processes are usually required in order to use the components. A milling process is often used to create functional surfaces. The paper shows whether the additive manufacturing process has an influence on the milling process. For this purpose, additive manufacturing processes using powder and laser (SLM), powder and arc (3DPMD), as well as wire and arc (WAAM) of the same material are compared. Based on the microstructure and the different mechanical properties, the component properties are compared with each other and with conventional sheet metal. For this purpose, samples are cut from additively manufactured components and milled under identical conditions. The temperature and the milling forces are measured and evaluated. It is shown that the additive manufacturing process results in significant differences in machinability and that the mechanical properties alone do not provide sufficient information about the machinability.

**Keywords:** additive manufacturing; process qualification; post-process; milling force; microstructure; powder; laser; wire; SLM; 3DPMD; WAAM



**Citation:** Laue, R.; Colditz, P.; Möckel, M.; Awiszus, B. Study on the Milling of Additive Manufactured Components. *Metals* **2022**, *12*, 1167. <https://doi.org/10.3390/met12071167>

Academic Editor: Amir Mostafaei

Received: 29 April 2022

Accepted: 1 July 2022

Published: 8 July 2022

**Publisher's Note:** MDPI stays neutral with regard to jurisdictional claims in published maps and institutional affiliations.



**Copyright:** © 2022 by the authors. Licensee MDPI, Basel, Switzerland. This article is an open access article distributed under the terms and conditions of the Creative Commons Attribution (CC BY) license (<https://creativecommons.org/licenses/by/4.0/>).

## 1. Introduction and Motivation

The additive manufacturing of components is increasing in prevalence. The global market in the field of additive manufacturing processes has increased significantly within just a few years. In 2014, the revenue generated by additive manufacturing amounted to USD 4.1 billion. In 2019, this has increased to USD 10.4 billion. A further growth in global sales is expected [1,2]. In metal-based additive manufacturing processes, workpieces are created by applying material layer by layer from a mostly shapeless base material (wire or powder). Thus, these processes usually have a much lower material input than conventional processes. Furthermore, additive manufacturing enables the production of components with small post-processes and with high flexibility in terms of product variants and individuality.

Although the processes are continuously being developed and improved, process-related shape deviations and the surface properties make post-processing through machining for the production of functional surfaces mostly unavoidable.

There are many studies that examine the machining of additive manufactured components. Due to their extremely interesting properties for research, titanium and nickel alloys have been considered in numerous works [3,4]. In this regard, the article “Review on machining of additively manufactured nickel and titanium alloys” [3] provides a very good overview of the research work carried out at the present time. Usually, the influence of the characteristic workpiece properties (hardness, microstructure and anisotropy) resulting from the AM process on the subsequent machining process is discussed. It is also clear from the compilation of research that the machinability of AM-produced components differs significantly from that of comparable conventional semi-finished products. Furthermore, there are also studies on the machinability of additively manufactured components which also use the austenitic steelmaking material 316L [5–7]. Among other things, these are

concerned with the process-related influences on the cutting forces [5], on the wear properties of the cutting tool and the final component properties (surface roughness) [6,7]. The properties of a part produced by a specific additive process (e.g., LAM [6], SLM [8] or WAAM [9]) are usually compared with those of conventional wrought alloys.

In contrast to the previous studies, this work deals with the comparison of several different additive manufacturing processes and their influence on the machining process. Here, processes with different forms of energy input (laser and arc) and starting material (powder and wire) are investigated. A special unique characteristic here is that both powder and wire were produced from the same starting material. In addition, several factors (milling forces, temperature, chip shape, surface roughness) are taken into account for the comparison in order to evaluate machinability in combination with the material properties.




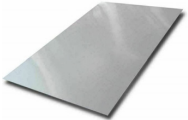
The aim of this work is a manufacturing-process-dependent evaluation of the machinability of various additively manufactured components. For this purpose, the additively manufactured specimen and a conventionally manufactured semi-finished product made of an identical material are chosen for the study. The experimental investigations will provide information about the respective material behavior during the machining process in order to be able to better control the post-processing in the future and thus make it more economical.

## 2. Materials and Methods

### 2.1. Production of the Reference Components

In the study, components produced by selective laser melting (SLM), wire arc additive manufacturing (WAAM), 3D plasma-metal deposition (3DPMD) and a conventional sheet are compared. SLM and 3DPMD are powder-based processes, whereas WAAM is a wire-based process. Further information in regards to the named processes is given in the following publications [2,7,10]. The reference material for comparison is considered from a cold rolled blank. The general characteristics of the different additive manufacturing processes are shown in Table 1.

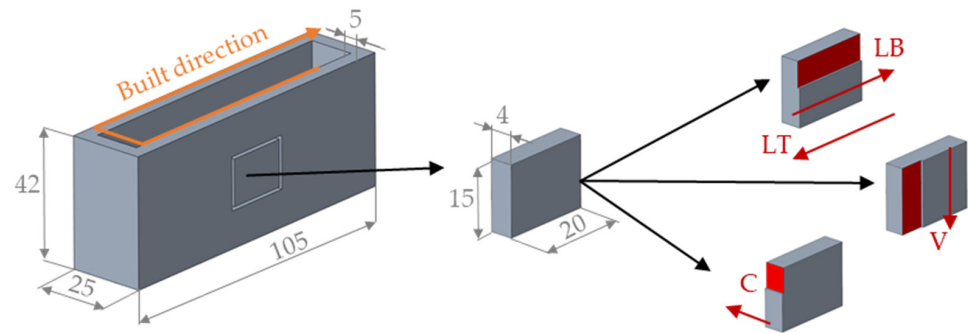
**Table 1.** Characteristics of the additive processes investigated in the study.

Manufacturing Process	SLM	WAAM	3DPMD	Sheet Metal
Material			316L (1.4403)	
Initial state	Powder (30–63 µm)	Wire (Ø 1.2 mm)	Powder (50–125 µm)	Sheet (cold rolled)
Melting source	Laser	Arc	Arc	-
Layer height/sheet thickness	0.06 mm	1.70 mm	0.97 mm	6.00 mm
Process time/reference component	231.3 min	13.5 min	22.5 min	Not specified
Reference component				

A technically relevant austenitic stainless steel (1.4403) was used for the study. The starting material was therefore identical for all processes, so that the differences in properties and machinability were only due to process-related influences, in particular the type of energy input and the shape of the starting material. The selected particle dimensions and the used wire diameter were process-dependent; their determination originated from previous investigations [2,11].

A rectangular circumferential wall was selected as the specimen (see Figure 1). With the different manufacturing processes, different mechanical and thermal properties in the component occurred [12]. Thus, the properties along the different wall directions had

to be considered. As can be seen in Figure 1, the upright direction in the specimen wall (vertical—V) was investigated, as well as the forward direction of the structure (lengthwise towards—LT) and in the opposite direction (lengthwise backwards—LB). Furthermore, the direction transverse to the specimen wall (crosswise—C) was investigated. The following figure also serves to illustrate the direction-dependent specimen preparation. The designations mentioned here will continue to be used in the following investigation.



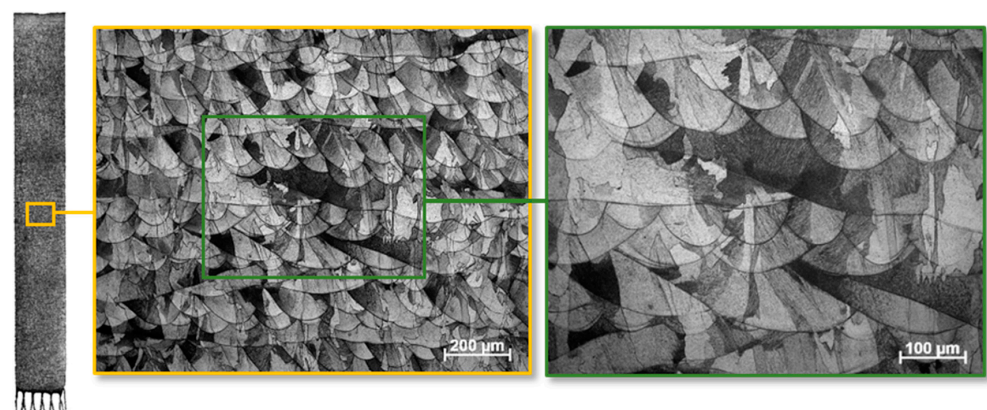
**Figure 1.** Dimensions of the reference component and investigated specimen directions.

First, the initial properties of the manufactured reference components were examined (microstructure and strength). Then, the specimens were prepared in the way to achieve identical starting conditions for the machining process.

## 2.2. Initial State of the Microstructure

Due to the different manufacturing processes, the samples have different initial states, which must be known for the evaluation of machinability. First, the different microstructures of the components were considered before machining and then the mechanical properties were compared [13]. For this purpose, the initial geometry was cut open crosswise to the wall, embedded and prepared accordingly for microscopy. The figures were made by a Zeiss inverted microscope, Axio Observer 3 materials and an Axiocam.

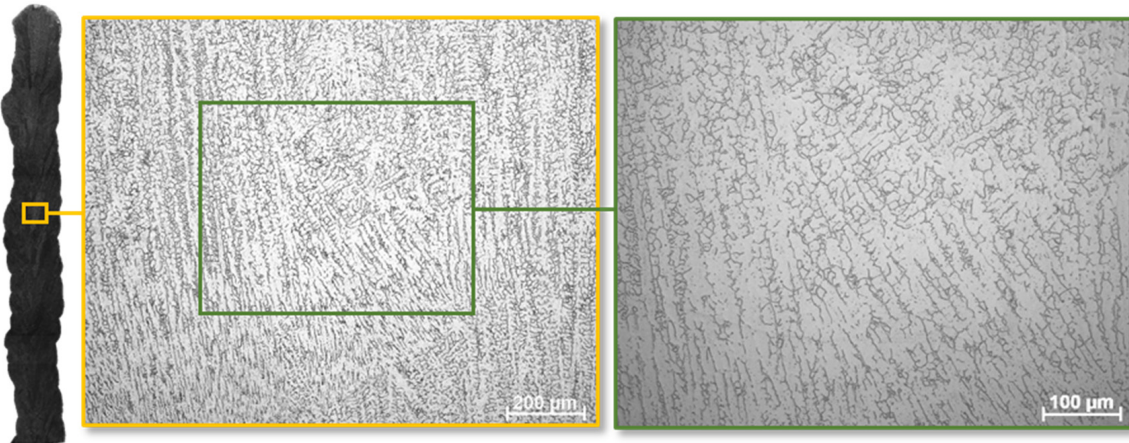
The micrograph of the SLM specimen is shown in Figure 2. It is characterized by compact, lenticular structures with dimensions of ca. 100  $\mu\text{m}$ . These structures characterize the heat-affected zone and are larger than the original powder particle size of 30–63  $\mu\text{m}$  and the spot diameter of the laser (80  $\mu\text{m}$ ). Consequently, the particles have connected together in the local weld pool and, in addition, neighboring welds have also connected. Subsequent layer application caused the already existing layers to experience renewed heat input; this resulted in a kind of heat treatment of the underlying layers and caused a microstructure to form across the boundaries of the weld lenses. This is illustrated by grain boundaries that have formed across several weld lenses.



**Figure 2.** Microstructure of the SLM component.

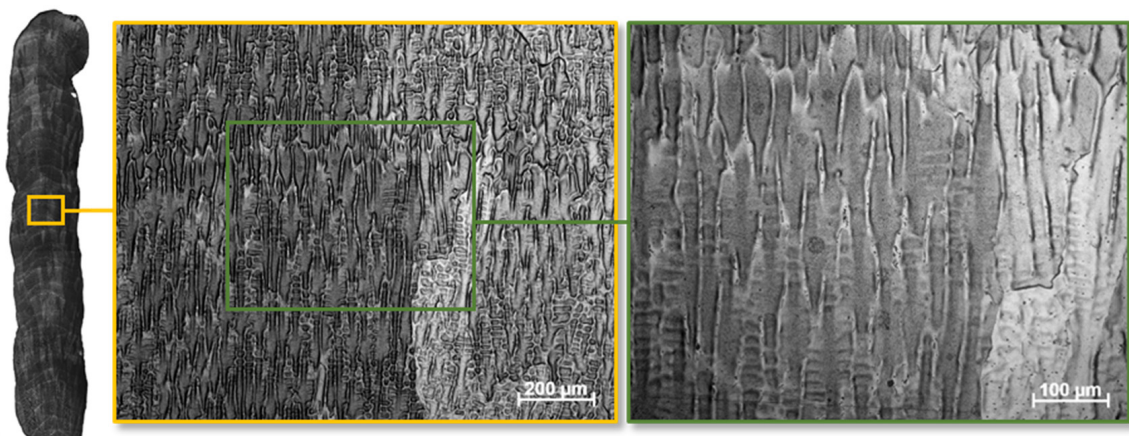


The micrograph of the WAAM wall in Figure 3 shows a typical as-cast microstructure with dendrites, as also found in weld seams. Due to this structure, individual grains are sometimes not clearly recognizable. The long dendrites show a uniform orientation. In addition, the microstructure probably exhibits  $\delta$ -ferrite or precipitates deposited in the region of the grain boundaries [14].



**Figure 3.** Microstructure of the WAAM component.

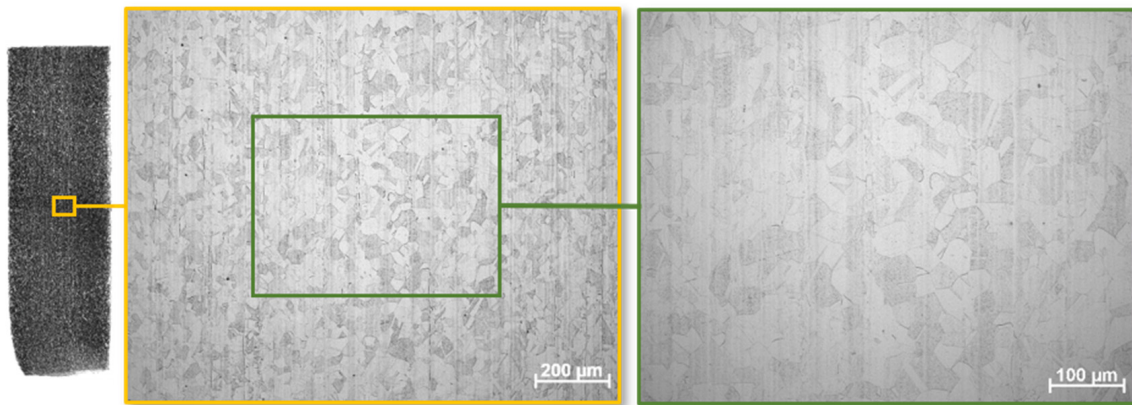
The micrograph of the 3DPMD sample (Figure 4) shows no clearly recognizable grain structure. The original powder particles of 50–125  $\mu\text{m}$  are still visible. These have not bonded together during the manufacturing process in such a way that a uniform microstructure could form. It is possible that the microstructure formation was disturbed by a boundary layer (oxide layer) between the individual particles. The formation of oxide layers cannot be completely avoided despite the use of inert gas. The powder particles show a long and distorted shape due to the process. A grain-like structure can be seen within the particles.



**Figure 4.** Microstructure of the 3DPMD component.

The micrograph in Figure 5 shows the microstructure of a conventionally produced cold rolled sheet. It depicts an austenitic microstructure with homogeneous grains. Vertical segregation lines can be clearly seen. These are created during primary casting of the material and are aligned by the rolling process in sheet production [15].

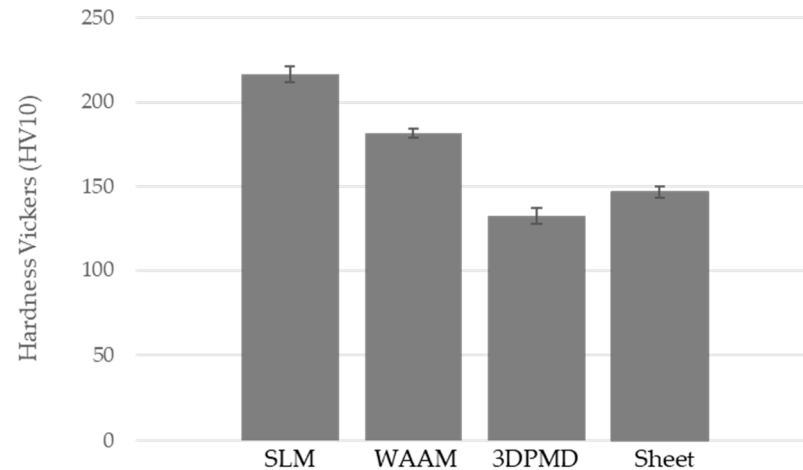




**Figure 5.** Microstructure of a sheet metal (reference material).

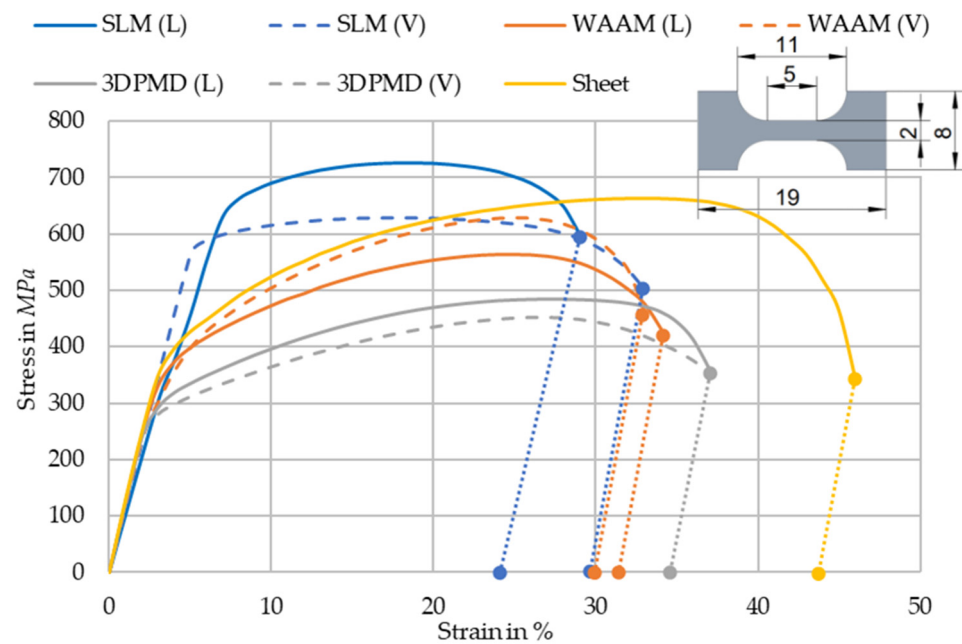
### 2.3. Mechanical Properties of the Reference Component

In addition to the microstructure, the hardness and the strength of a material are influencing parameters in the machining process [5]. The Vickers hardness test (HV 10) was performed on the previously shown microsection specimen with a Zwick hardness tester 3212 (ZwickRoell GmbH & Co. KG, Ulm, Germany). These were thereby measured in the vertical direction. The diagram (Figure 6) reflects the average value (mean value) of hardness for the different manufacturing processes. The hardness test shows that the 3DPMD specimens have the lowest hardness at approx. 133 HV 10. Above this is the 316L reference material with approx. 147 HV 10. Much higher hardness values are measured for the WAAM specimens (approx. 181 HV 10) and the SLM specimens (approx. 216 HV 10).



**Figure 6.** Vickers hardness (HV 10) of the different additive manufacturing processes.

The hardness provides pointwise information about the mechanical properties. Due to the significantly different microstructures, the stress-strain diagram was also determined by tensile tests, which were performed on the tensile testing machine Galdabini Quasar 50 (Galdabini SPA, Cardano al Campo, Italy). Aside from this, micro tensile specimens (specimen dimensions in Figure 7) were separated from the component and tested. Since the direction-dependent mechanical properties are also to be investigated in the further course, the micro tensile specimens were taken lengthwise (L) and vertical (V) to the wall (see Figure 1). Sampling crosswise (C) was not possible due to the thin wall thickness. For the reference material made of sheet metal, the samples were taken along the rolling direction. Samples were not taken crosswise to the rolling direction. On the one hand, this comparison is not part of the investigation; on the other hand, poorer mechanical properties are expected here. The results are shown in Figure 7.



**Figure 7.** Tensile tests of the different additive manufacturing processes.

It can be seen that the 3DPMD specimens have very high elongation at break regardless of the specimen direction taken, but the lowest tensile strength. The WAAM specimens have slightly higher tensile strength, but also lower elongation at break. The reference material has the highest elongation at break and slightly higher tensile strength than the WAAM specimens. The SLM specimens have the highest tensile strength. They also have the lowest elongation at break.

### 3. Experimental Investigation

#### 3.1. Sample Preparation

Due to the investigations of the mechanical properties, especially the results from the tensile tests, it becomes clear that the additive manufacturing of the specimens results in different material properties in different directions (for example, lengthwise towards built direction and upright in the specimen wall). Accordingly, the milling properties are also studied in different directions. For this purpose, samples are cut out from the reference components in horizontal and vertical directions (in each case in the direction of the layer structure and opposite and transverse to the wall), as shown in Figure 8.

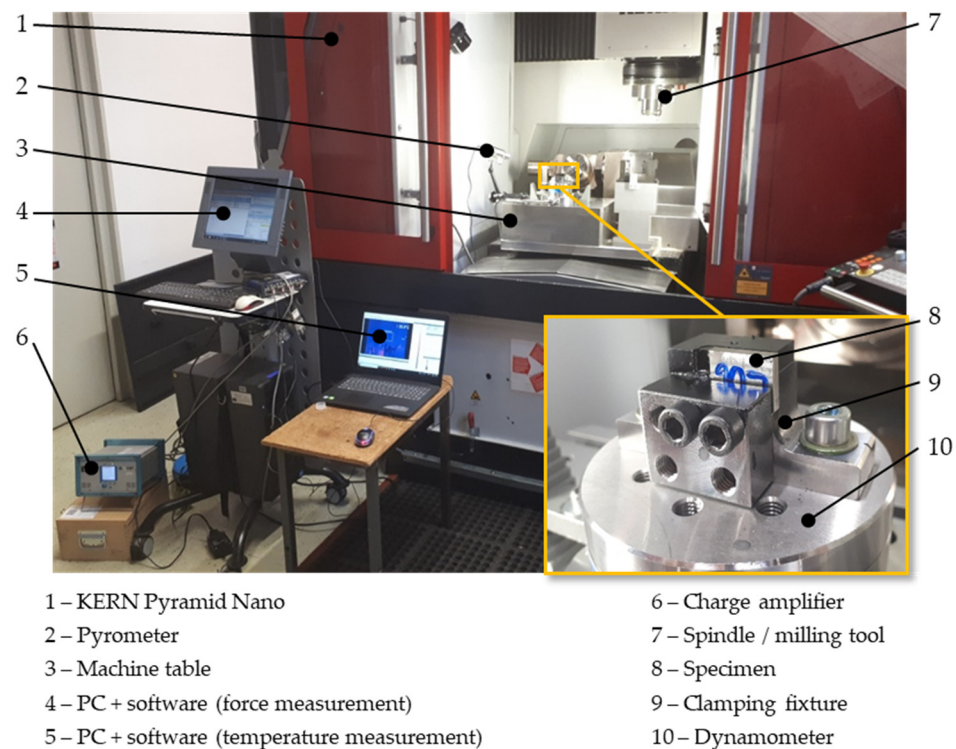


**Figure 8.** Sequence of sample preparation.

The height of the specimens was identical in the center of the component for all processes. Subsequently, the specimens were machined to remove the structured surface from the layers of the additive process and to obtain equal dimensions of the specimens. This firstly ensured that the specimen could be clamped correctly and secondly produced a uniform specimen volume and geometry so that the results could be compared.

### 3.2. Experimental Set-Up

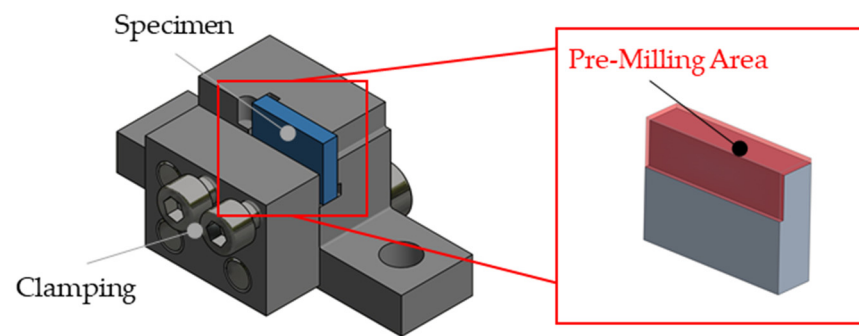
The milling tests (Figure 9) were performed on the high-precision milling machining center KERN Pyramid Nano (CNC-controlled) (KERN Microtechnik GmbH, Eschenlohe, Germany). For machining, an end mill was selected whose diameter is small enough to be in full engagement with the 4 mm wall (direction C) and which nevertheless has sufficient stability to chip the entire test surface. The desired chip depth and width must also be realized. Therefore, an end mill in a long design was suitable. In addition, the material suitability of the tool must be considered. The decision was made to use a solid carbide high-performance milling cutter specially designed for machining stainless steel, which has a diameter of 6 mm, three cutting edges, cutting tips with 45° chamfer and a coating adapted to INOX machining. The milling parameters follow the recommendations of the tool maker, so that the milling cutter rotates at 4000 rpm and has a feed rate of 400 mm/min. Due to the large number of specimens (6 specimens per direction equals 18 specimens per process and 54 specimens in total) and the time-consuming sampling procedure, the input parameters were not varied in this first study.



**Figure 9.** Experimental set-up including measurement technology for the milling tests.

The specimen was fixed in the clamping fixture (Figure 10 left) with uniform torque (10 Nm) and then machined in the clamped condition. Prior to the tests, a minimum amount of material was removed from the top and front surfaces (see Figure 10 right). This ensures that all specimens have an identical position in the experimental tests and that the reduction in chip volume is identical.



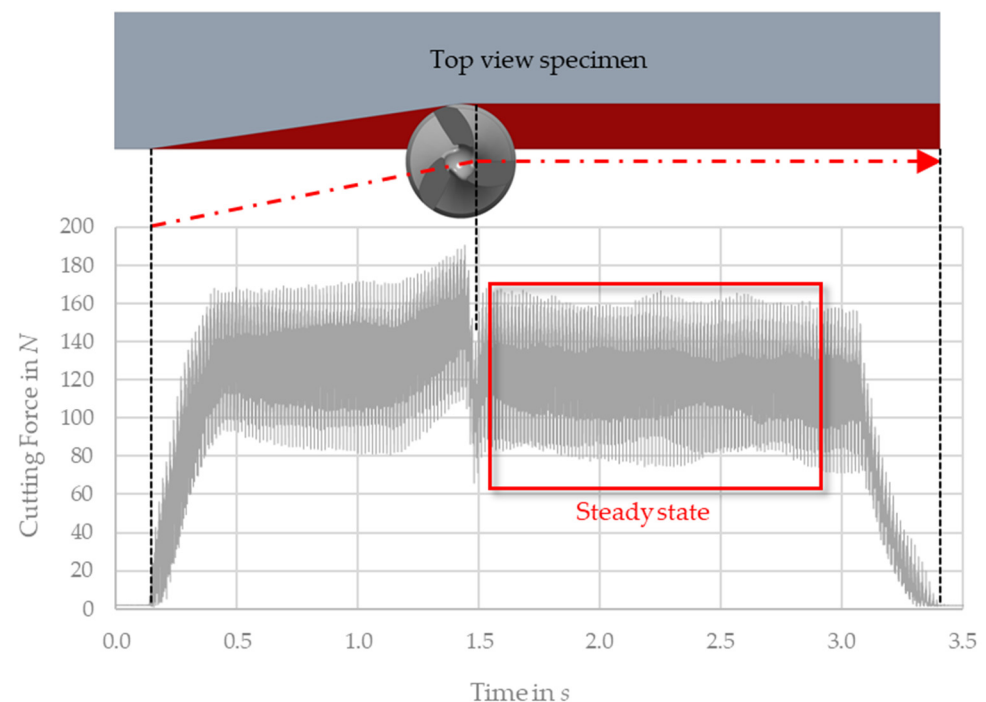


**Figure 10.** Clamping fixture (left) and pre-milling (right).

### 3.3. Measurement Results

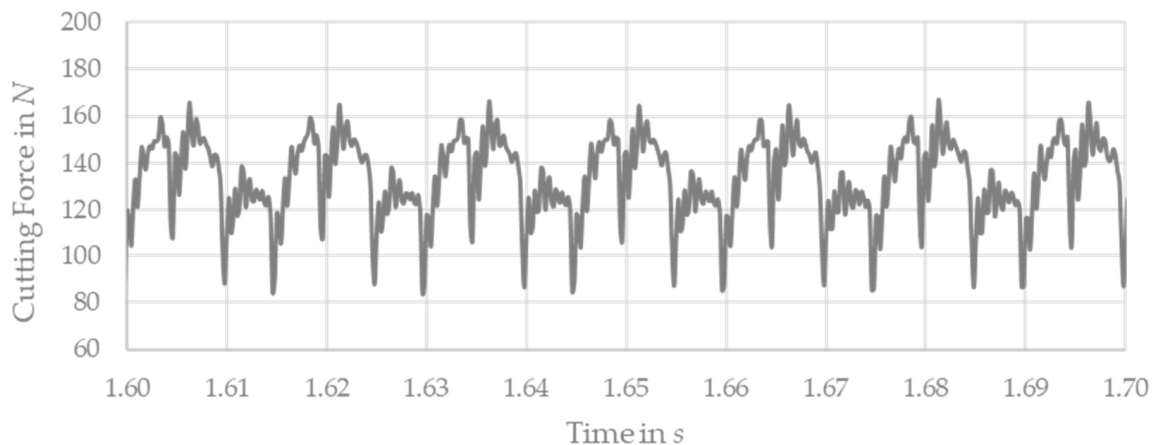
During the execution of the machining tests, the forces and the temperature were measured. To determine the force, a stationary piezoelectric four-component dynamometer (type 9272 from Kistler) was used, to which the clamping device was attached.

Figure 11 shows an example of the measured milling force during a single test. At the beginning of the test, the force increases sharply from approx. 0.2 s onwards. This increase marks the contact from the cutter at the material. The increase in the range of 0.4 s to 1.4 s is due to the increasing cutting volume during the oblique feed of the cutter into the material. After a short dwell time after reaching the specified chip width (decrease in cutting force at  $t \approx 1.5$  s), the cut began with a constant chip cross-section and a constant feed rate and a quasi-steady state (shown in red) was established. The cutter exit becomes apparent from approx. three seconds of the process time by a steep drop in the force curve.



**Figure 11.** Exemplary representation of the milling force during the machining (3DPMD).

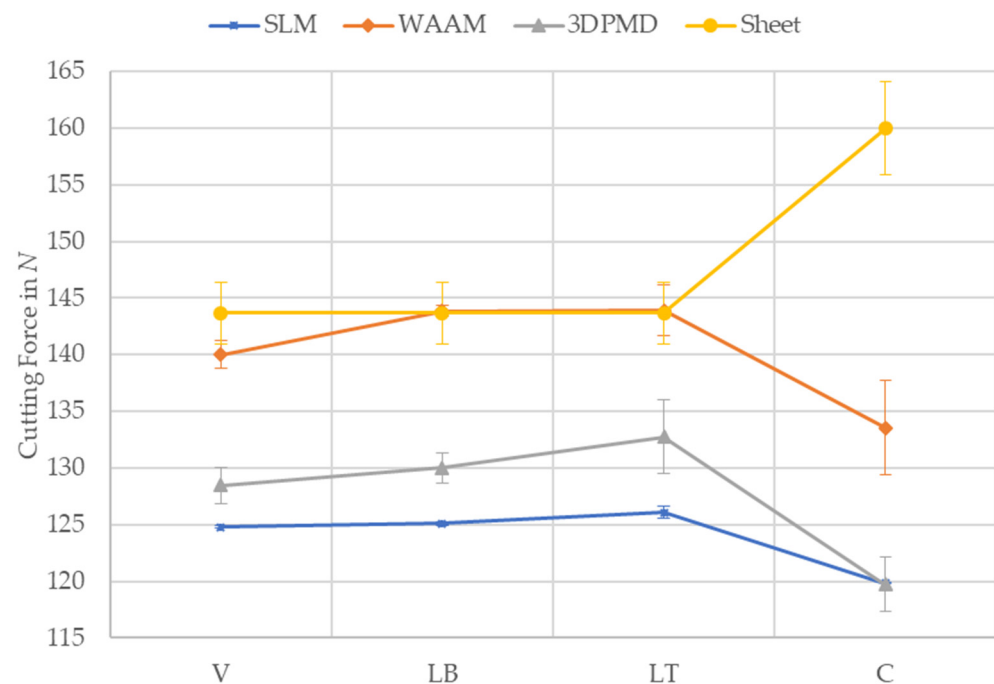
For further evaluation of the tests, only the quasi-static range (between 1.6 and 2.8 s of the test time) was considered. Due to the sample preparation and the process control, identical boundary conditions were present during this range for all tests. During the quasi-static range, the force changes periodically around an average value, as shown in Figure 12.



**Figure 12.** Force in the quasi-static range.

The measurement repetition frequency of the dynamometer is 4800 Hz. Since this is considerably higher than the rotational frequency of the cutter (66.67 Hz), the measurement technique resolves the variations of the cutting forces very accurately. The varying cutting forces result from the changing chip cross-sections during the milling operation. This can be seen in all the tests. The periodic variation occurs around an average value. Therefore, the measurement results during the steady state are mean values, which is permissible since only the relative differences of the measurement results are considered in this study.

At least five tests were carried out for each process, which were then averaged. For the comparison of the results, the five individual trend lines of all tests within a test group with uniform machining direction and uniform manufacturing process are combined to a mean milling force (see Figure 13). The maximum deviations from the mean value are shown in the diagram. The deviations result from the heating during milling and from the different initial material conditions (powder, wire). In addition to the additively manufactured samples, reference material from a sheet was also examined.



**Figure 13.** Mean milling force in the steady state area.

In general, the SLM specimens show the lowest cutting force overall. This is almost identical for the different directions (V, LB and LT), only the direction crosswise to the wall (C) is approx. 5 N lower. Overall, the specimens produced by SLM have the most homogeneous properties. Furthermore, it can be seen in the SLM specimens that there is only a minimal variation in the milling force in the steady state area.

The cutting forces of the 3DPMD specimens are slightly higher than the SLM specimens (approx. 5 N). On the one hand, it is clear that the milling force changes depending on the direction (compare V with LB/LT). On the other hand, the milling force is dependent on the feed direction of the additive production (comparison LB and LT). It can be seen that the milling force is greater against the feed direction in the manufacturing process. Furthermore, the milling force across the wall is about 10 N lower than in the wall plane. In addition, it is clear that compared to the SLM specimens, the milling forces vary significantly more in the steady state area.

The results of the WAAM specimens show no difference in milling force along the specimen wall (LB and LT). However, there is a small difference lengthwise and vertical to the specimen wall, as well as a large difference across the wall, which is most pronounced together with the results of the 3DPMD specimens. The change in force during milling in the steady state area is comparable to the change in the 3DPMD specimens and is clearly pronounced. Furthermore, the milling force of the WAAM specimen is on a level with the reference specimen made of sheet material and requires the highest milling force.

The milling force of the specimen made of sheet metal has no influence in the sheet plane ( $V = LB = LT$ ), only a very strong deviation crosswise to the sheet plane (sheet thickness direction). The reason for this is the forming of the rolled sheet. In contrast to the additively manufactured specimens, the milling force increases significantly here (approx. 15 N). In addition, the largest increase in milling force during the test can be seen with the specimens.

Overall, the additively manufactured specimens show a small deviation of the milling force in V, LB and LT directions, compared to the crosswise direction C to the specimen wall. SLM has the lowest milling force, 3DPMD slightly more and on a level are WAAM and the sheet material.

A spot finder pyrometer was used for the temperature measurement. This is a combination of pyrometer and infrared camera. Before the temperature measurements, the corresponding samples are painted with a matte black spray in order not to falsify the measurement by reflection from the smooth sample surface. The actual prevailing temperatures are higher than the measured values because the measurement is not possible exactly in the intervention point with the chosen experimental set-up. The highest measured temperature in the measuring range occurred at the milling cutter, which at this point had already made about half a revolution from the actual warmest point. The measured process temperatures show that all processes have a similar temperature profile. Differences with regard to heat development are shown by the WAAM samples. They are on a par with the reference material. The maximum temperatures of 3DPMD and SLM are on a similar level, about 10 °C below WAAM, with SLM showing slightly higher measured values. The average temperature curves by manufacturing process are shown in Figure 14. The small difference in temperature is nevertheless serious, since the milled path is only very small. It can be seen that the cooling of the 3DPMD sample is the fastest; this suggests that the heat input is the lowest. Consequently, the difference would be significantly greater for longer milling processes.

Figure 15 shows the chips of the individual tests. Since the machining conditions in the process differ only slightly, no significant difference in shape, color or size can be detected in the chips. All the chips sampled are crumbled chips with no discernible tempering color.



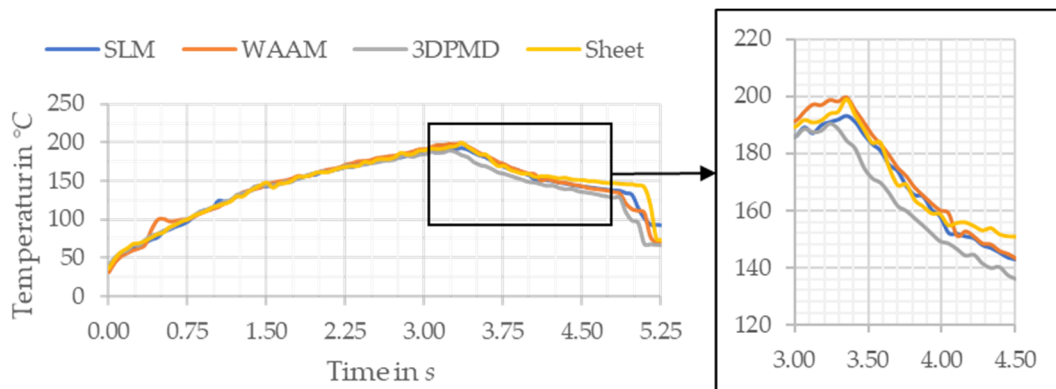


Figure 14. Averaged temperature curves during the machining process.

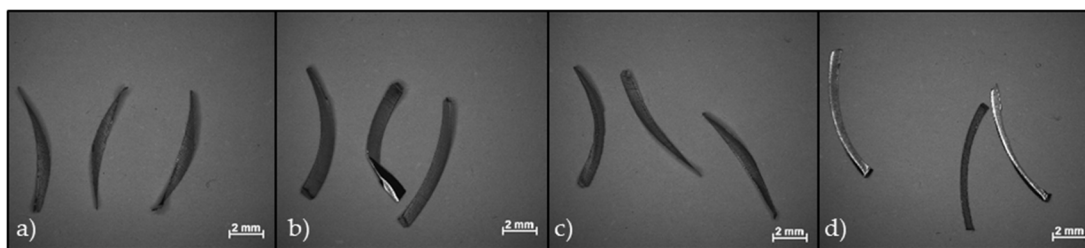


Figure 15. Chips of the milling process of (a) SLM, (b) WAAM, (c) 3DPMD, (d) sheet metal.

After the machining tests, the resulting surfaces were characterized using an optical laser scanning microscope (Keyence K-X3000). Here, the entire surface topography was recorded via focus variation and the measurement sections were placed on the recorded surface. The roughness (see Figure 16) of the milled surfaces was evaluated as a comparison criterion.



Figure 16. Rz values of the milled specimens by direction and AM process.

The measured differences between the individual manufacturing processes and the removal direction are very small. The values of the roughness are in the transition range between the usual and fine manufacturing accuracy in milling (approx. Rz 10) and vary by a maximum of 2 μm. Consequently, the additive production has no significant influence on the surface roughness.

#### 4. Discussion

Within the scope of the study, data were presented before, during and after the machining process, which will now be considered coherently.

The samples from SLM have a very uniform microstructure and there is a connection of the grains over several layers. As a result, the material has almost isotropic properties, which is clearly evident in the direction-independent hardness and milling force. The low milling forces are favored by the low elongation at break and the lenticular structure. Whereas the high hardness will have a negative effect on the closure of the mill.

The 3DPMD material has the lowest measured hardness, which is lower than the hardness value of the reference material. As a result, material heats up the least during cutting and cools down the fastest. In addition, the samples have the lowest tensile strength of the additive processes, but high elongation at break. The reason for this is the incomplete bonding of the grains of the individual layers. This is also the reason for the low cutting force, which is only slightly higher than that of the SLM samples. Another characteristic of the 3DPMD specimens is the large anisotropy of the material, which can be clearly seen in the milling forces. This can be explained by the microstructure and the macrostructure, in particular the layered structure of the specimens. The applied particles are highly distorted and thus provide the directional dependence of the mechanical properties. This also exists in the feed direction and in the opposite direction of the layer structure (LB and LT).

The WAAM samples also exhibit an orientation in the microstructure, resulting in low directional dependence of the mechanical properties. Furthermore, together with the reference material, these specimens possess the highest cutting forces. In contrast, however, WAAM has significantly lower hardness than the SLM specimens. This contradiction is due to the local microstructure composition. Especially in boundary areas between the applied layers, a higher concentration of harder oxide layers and silicates could be present. These have a negative effect on machinability over the entire surface, but cannot be detected by conventional hardness testing.

The investigations show that the machining process represents a system with several overlapping influencing variables. The microstructure resulting from the manufacturing process is mainly responsible for the machinability of the respective sample. While WAAM and 3DPMD have a continuous feed direction in the printing process, in the SLM process, directional independence is created by the 71° angular laser offset per layer. Furthermore, it is shown that the large particle size in 3DPMD and the possible formation of oxide layers at the particle boundaries prevent uniform microstructure formation and result in low milling forces. The wire-based WAAM process produces a material with properties that are most similar to the properties of the sheet material.

From the data generated and the relationships established, it is clear that components produced by SLM have the best machining properties. The parts produced by WAAM have the least favorable machining conditions and the 3DPMD samples are in between. Although the 3DPMD samples have opposite mechanical properties (tensile strength, elongation at break and hardness) compared to the SLM samples, the samples of both materials are very machinable.

When comparing the processes, it should further be noted that the fabrication of the SLM component requires a significantly higher (10×) process time and has the highest powder quality requirements. In addition, the installation space is limited by the machine size, whereas 3DPMD and WAAM can be manufactured using robots.

#### 5. Summary and Outlook

In the presented study, the machining of specimens produced by different additive processes was investigated. For this purpose, information was obtained before, during and after the machining process, which is summarized quantitatively in Table 2.

**Table 2.** Qualitative overview of the results.

	SLM	WAAM	3DPMD	Sheet Metal
Microstructure	Lenticular	Dendritic	Elongated	Homogeneous
Hardness	++	+	--	–
Tensile strength	+	–	--	–
Elongation at break	--	–	+	++
Force during milling	--	+	–	+
Temperature	+	+	–	+
Surface roughness	–	–	–	–

At the beginning of the investigation, the initial condition of the samples was first analyzed. It was found that differences in the microstructure became visible as a result of the manufacturing process, which was also evident in the mechanical properties. Subsequently, the specimens were prepared in such a way that identical conditions prevailed during the tests in order to obtain comparable results. During the machining tests, the force and temperature were measured and then processed for evaluation.

Based on the investigation, it was determined that the machining properties of additively manufactured components depend on the manufacturing process and affect the downstream manufacturing process. In addition to different milling forces, the samples also have different anisotropies and temperatures. The force anisotropy shown in the table describes the forces within the additively manufactured wall or within the sheet metal plane. In the study presented here, the SLM process shows the best properties in terms of machinability, followed by 3DPMD and WAAM.

For a cutting force calculation, the additive manufacturing process and the milling direction in relation to the build-up direction must therefore also be considered. A conventional cutting force calculation for the materials cannot be used.

For future investigations, the influence of varying input parameters during milling (speed, feed, etc.) should be analyzed in detail. In addition, the effects of additive processes on tool wear during machining should be investigated in more detail within the context of long-term tests.

**Author Contributions:** Conceptualization, R.L.; methodology, R.L., P.C. and M.M.; software, M.M.; validation, M.M., R.L.; formal analysis, R.L., M.M. and P.C.; investigation, M.M.; resources, B.A.; data curation, M.M.; writing—original draft preparation, R.L.; writing—review and editing, P.C.; visualization, M.M., R.L. and P.C.; supervision, B.A.; project administration, B.A.; funding acquisition, B.A. All authors have read and agreed to the published version of the manuscript.

**Funding:** This research was funded by the DAAD (German Academic Exchange Service) project code number 57459939 and by the Deutsche Forschungsgemeinschaft (DFG, German Research Foundation)—491193532.

**Institutional Review Board Statement:** Not applicable.

**Informed Consent Statement:** Not applicable.

**Data Availability Statement:** The data presented in this study are available on request from the corresponding authors.

**Acknowledgments:** The authors would like to thank the professorship welding technology and the professorship micromanufacturing technology of the Chemnitz University of Technology.

**Conflicts of Interest:** The authors declare no conflict of interest.



## References

1. Smartech Analysis, 2020 Additive Manufacturing Market Outlook. Available online: [www.smartechanalysis.com/news/2019-additive-manufacturing-market-growth/](http://www.smartechanalysis.com/news/2019-additive-manufacturing-market-growth/) (accessed on 29 April 2022).
2. Hoefler, K.; Haelsig, A.; Mayr, P. Arc-based additive manufacturing of steel components—comparison of wire- and powder-based variants. *Weld World* **2018**, *62*, 243–247. [[CrossRef](#)]
3. Oyelola, O.; Crawforth, P.; M'Saoubi, R.; Clare, A.T. Machining of Additively Manufactured Parts: Implications for Surface Integrity. *Procedia CIRP* **2016**, *45*, 119–122. [[CrossRef](#)]
4. Khanna, N.; Zadafiya, K.; Patel, T.; Kaynak, Y.; Rashid, R.A.R.; Vafadar, A. Review on machining of additively manufactured nickel and titanium alloys. *J. Mater. Res. Technol.* **2021**, *15*, 3192–3221. [[CrossRef](#)]
5. Montevicchi, F.; Grossi, N.; Takagi, H.; Scippa, A.; Sasahara, H.; Campatelli, G. Cutting Forces Analysis in Additive Manufactured AISI H13 Alloy. *Procedia CIRP* **2016**, *46*, 476–479. [[CrossRef](#)]
6. Gong, Y.; Li, P. Analysis of tool wear performance and surface quality in post milling of additive manufactured 316L stainless steel. *J. Mech. Sci. Technol.* **2019**, *33*, 2387–2395. [[CrossRef](#)]
7. Vayre, B.; Vignat, F.; Villeneuve, F. Metallic additive manufacturing: State-of-the-art review and prospects. *Mech. Ind.* **2012**, *13*, 89–96. [[CrossRef](#)]
8. Greco, S.; Kieren-Ehse, S.; Kirsch, B.; Aurich, J.C. Micro milling of additively manufactured AISI 316L: Impact of the layerwise microstructure on the process results. *Int. J. Adv. Manuf. Technol.* **2021**, *112*, 361–373. [[CrossRef](#)]
9. Lopes, J.G.; Machado, C.M.; Duarte, V.R.; Rodrigues, T.A.; Santos, T.G.; Oliveira, J.P. Effect of milling parameters on HSLA steel parts produced by Wire and Arc Additive Manufacturing (WAAM). *J. Manuf. Processes* **2020**, *59*, 739–749. [[CrossRef](#)]
10. Brandl, E.; Baufeld, B.; Leyens, C.; Gault, R. Additive manufactured Ti-6Al-4V using welding wire: Comparison of laser and arc beam deposition and evaluation with respect to aerospace material specifications. *Phys. Procedia* **2010**, *5*, 595–606. [[CrossRef](#)]
11. Taufek, T.; Manurung, Y.H.P.; Lüder, S.; Graf, M.; Salleh, F.M. Distortion Analysis of SLM Product of SS316L using Inherent Strain Method. *IOP Conf. Ser. Mater. Sci. Eng.* **2020**, *834*, 12011. [[CrossRef](#)]
12. Lewandowski, J.J.; Seifi, M. Metal Additive Manufacturing: A Review of Mechanical Properties. *Annu. Rev. Mater. Res.* **2016**, *46*, 151–186. [[CrossRef](#)]
13. Pan, Z.; Feng, Y.; Liang, S.Y. Material microstructure affected machining: A review. *Manuf. Rev.* **2017**, *4*, 5. [[CrossRef](#)]
14. Colditz, P.; Graf, M.; Hälsig, A.; Härtel, S.; Prajadhama, K.P.; Manurung, Y.P.; Awiszus, B. Experimental Investigation of Different WAAM (Wire-Arc Additive Manufacturing) Processes and Their Influence on the Component Properties and Formability. In *The Minerals, Metals & Materials Series, Forming the Future*; Daehn, G., Cao, J., Kinsey, B., Tekkaya, E., Vivek, A., Yoshida, Y., Eds.; Springer International Publishing: Cham, Switzerland, 2021; pp. 2853–2865.
15. Giertler, A. *Mechanismen der Rissentstehung und -Ausbreitung im Vergütungsstahl 50CrMo4 bei sehr Hohen Lastspielzahlen*; Berichte aus dem Institut für Eisenhüttenkunde: Aachen, Germany, 2020.